



The following Communications have been judged by at least two referees to be “very important papers” and will be published online at [www.angewandte.org](http://www.angewandte.org) soon:

P. García-Álvarez, D. V. Graham, E. Hevia, A. R. Kennedy, J. Klett, R. E. Mulvey,\* C. T. O'Hara, S. Weatherstone  
**Unmasking Representative Structures of TMP-Active Hauser and Turbo Hauser Bases**

D. Staack, A. Fridman, A. Gutsol, Y. Gogotsi\*, G. Friedman\*  
**Nanoscale Corona Discharge in Liquids Enabling Nanosecond Optical Emission Spectroscopy**

C. Hawner, K. Li, V. Cirriez, A. Alexakis\*  
**Copper-Catalyzed Asymmetric Conjugate Addition of Aryl Aluminum Reagents to Trisubstituted Enones: Construction of Aryl-Substituted Quaternary Centers**

K. W. Eberhardt, C. L. Degen, A. Hunkeler, B. H. Meier\*  
**One- and Two-Dimensional NMR Spectroscopy with a Magnetic-Resonance Force Microscope**

S. Wan, J. Guo, J. Kim, H. Ihee, D. Jiang\*  
**A Belt-Shaped, Blue-Luminescent and Semiconducting Covalent Organic Framework**

R. E. Jilek, M. Jang, E. D. Smolensky, J. D. Britton, J. E. Ellis\*  
**Structurally Distinct Homoleptic Anthracene Complexes  $[M(C_{14}H_{10})_3]^{2-}$ , M=Ti, Zr, Hf: Tris(arene) Complexes for a Triad of Transition Metals**

Dihydrogen Bonds

Vladimir I. Bakhmutov

Nanoparticles and Catalysis

Didier Astruc

## Books

reviewed by G. R. Desiraju \_\_\_\_\_ 7794

reviewed by M. S. Wong \_\_\_\_\_ 7795

In a recent publication, Krossing, Scherer, and co-workers reported interesting experimental results for homoleptic  $Ag^I$  acetylene complexes. In this Correspondence

the interpretation of the X-ray analysis and the claim of “pseudo-gas-phase conditions” in the solid state are questioned.

The comments of Krapp and Frenking are acknowledged, however, it is proposed that a detailed description of the nature of the metal–ligand bonding in the  $Ag^I$

acetylene complexes has to consider orbital interactions, in contrast to the electrostatic picture drawn by Krapp and Frenking.

## Correspondence

### Silver Acetylene Complexes (1)

A. Krapp, G. Frenking\* \_\_\_\_\_ 7796–7797

Comments on “Homoleptic Silver(I) Acetylene Complexes”

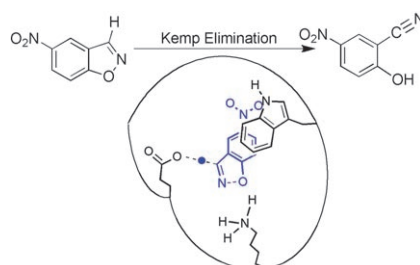
### Silver Acetylene Complexes (2)

D. Himmel, N. Trapp, I. Krossing,\*  
S. Altmannshofer, V. Herz, G. Eickerling,  
W. Scherer\* \_\_\_\_\_ 7798–7801

Reply



**Intelligent design:** The combination of computational design and directed evolution has allowed the creation and optimization of an artificial enzyme starting from a catalytically inactive protein scaffold. In this approach, glutamate, tryptophane, and lysine residues were introduced into a TIM barrel fold to yield an artificial enzyme for the Kemp elimination that was fine-tuned by directed evolution ( $k_{cat}/K_m = 2590 \text{ M}^{-1} \text{ s}^{-1}$ , see picture).



## Highlights

### Directed Evolution

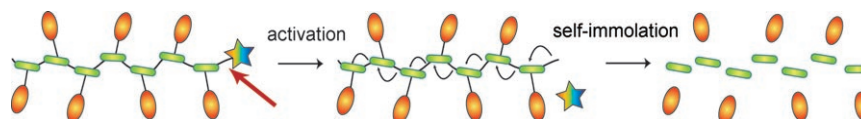
T. R. Ward\* \_\_\_\_\_ 7802–7803

Artificial Enzymes Made to Order:  
Combination of Computational Design  
and Directed Evolution

## Functional Materials

W. Wang, C. Alexander\* — 7804–7806

### Self-Immulative Polymers



**This message will self-destruct!** Polymers that can be triggered to disassemble in a sequential fashion following a single triggering event were described recently. The amplification effect after cleavage of an end group by an enzyme leads to the

spontaneous fragmentation of the polymer and the release of fluorescent reporters. The significance of these systems in terms of enzyme detection and drug release is discussed.

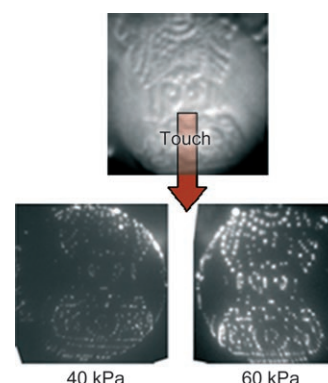
## Reviews

### Touch Sensors

V. Maheshwari, R. Saraf\* — 7808–7826

Tactile Devices To Sense Touch on a Par with a Human Finger

**Electronic skin:** Emulating the tactile sense of human touch will have a great impact on robotics. A new flexible thin film composed of nanoparticles and polyelectrolyte can feel texture on a par with a human finger. The picture shows how the pressing of a coin on such a sensor leads to a specific voltage distribution. Current research in nanomaterials and molecular electronics is described.



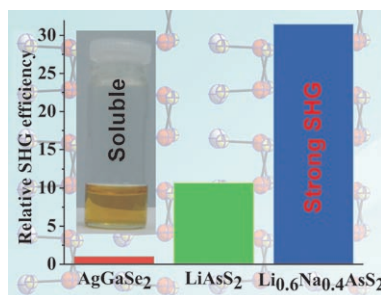
## Communications

### Direct-Gap Semiconductors

T. K. Bera, J.-H. Song, A. J. Freeman, J. I. Jang, J. B. Ketterson, M. G. Kanatzidis\* — 7828–7832



Soluble Direct-Band-Gap Semiconductors  $\text{LiAsS}_2$  and  $\text{NaAsS}_2$ : Large Electronic Structure Effects from Weak As...S Interactions and Strong Nonlinear Optical Response



**Bridging the gap:**  $\text{Li}_{1-x}\text{Na}_x\text{AsS}_2$  ( $x=0-1$ ) species are found to be a new class of polar direct-gap semiconductors, which display a strong second harmonic generator (SHG) response. The anomalous band-gap trend and their direct-band-gap nature was studied by calculations. The 1.6 eV direct energy gap of  $\text{LiAsS}_2$  coupled with its high solubility makes it promising as an efficient light harvesting component in solar cells.

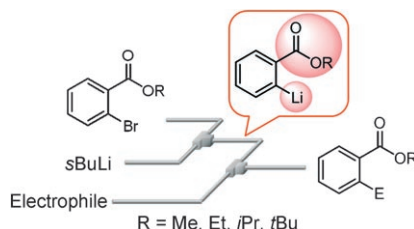
### For the USA and Canada:

ANGEWANDTE CHEMIE International Edition (ISSN 1433-7851) is published weekly by Wiley-VCH, PO Box 191161, 69451 Weinheim, Germany. Air freight and mailing in the USA by Publications Expediting Inc., 200

Meacham Ave., Elmont, NY 11003. Periodicals postage paid at Jamaica, NY 11431. US POSTMASTER: send address changes to *Angewandte Chemie*, Wiley-VCH, 111 River Street, Hoboken, NJ 07030. Annual subscription price for institutions: US\$ 7225/6568 (valid for print and

electronic / print or electronic delivery); for individuals who are personal members of a national chemical society prices are available on request. Postage and handling charges included. All prices are subject to local VAT/sales tax.

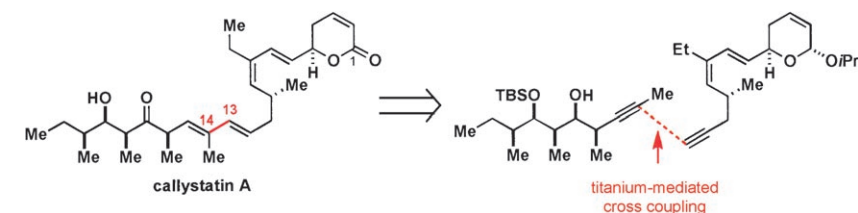
**Go with the flow:** An effective method for the generation and reaction of aryllithium compounds bearing an alkoxycarbonyl group is developed using microflow systems with very short residence times together with fast mixing and efficient temperature control. A wide range of alkoxycarbonyl groups including ethoxycarbonyl and methoxycarbonyl groups are tolerant of the microflow conditions.



### Microreactors

A. Nagaki, H. Kim, J.-i. Yoshida\* 7833–7836

Aryllithium Compounds Bearing Alkoxycarbonyl Groups: Generation and Reactions Using a Microflow System



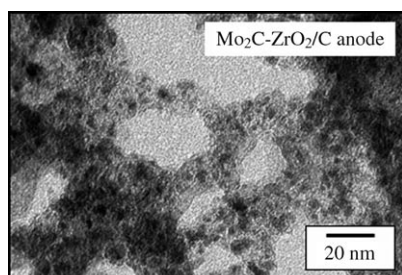
**Using a modular approach:** A concise synthesis of callistatin A has been developed. The modular pathway provides access to the highly unsaturated skeleton of the leptomyacin natural products by

using a complex titanium-mediated reductive alkyne-alkyne cross-coupling reaction as the key transformation (see scheme; TBS = *tert*-butyldimethylsilyl).

### Natural Product Synthesis

H. A. Reichard, J. C. Rieger, G. C. Micalizio\* 7837–7840

Total Synthesis of Callistatin A by Titanium-Mediated Reductive Alkyne-Alkyne Cross-Coupling



**Low temperature, high voltage!** Direct oxidation of hydrocarbon fuels, including methane, ethane, propane, and butane, occurs over Pt-free anodes in a proton-conducting fuel cell in the temperature range 100–300°C. A Mo<sub>2</sub>C–ZrO<sub>2</sub>/C anode (30 mg Mo<sub>2</sub>C–ZrO<sub>2</sub> per cm<sup>2</sup>) yields power densities equal to those obtained from Pt/C anodes (1–7 mg Pt per cm<sup>2</sup>) and generates higher open-circuit voltages than the Pt/C anodes.

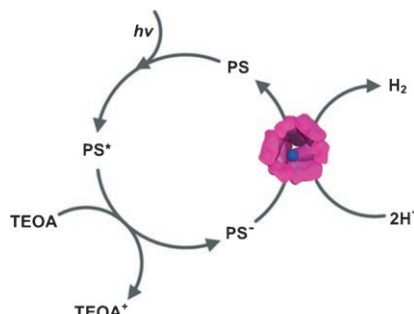
### Fuel Cells

P. Heo, K. Ito, A. Tomita, T. Hibino\* 7841–7844

A Proton-Conducting Fuel Cell Operating with Hydrocarbon Fuels



**Matter of size:** Platinum nanocluster formation inside protein cages (LiDps protein) was monitored by noncovalent mass spectrometry. The Pt clusters catalyze hydrogen formation in presence of an iridium photosensitizer (PS; see scheme, TEOA = triethanolamine), and their catalytic activity depends on the cluster size.



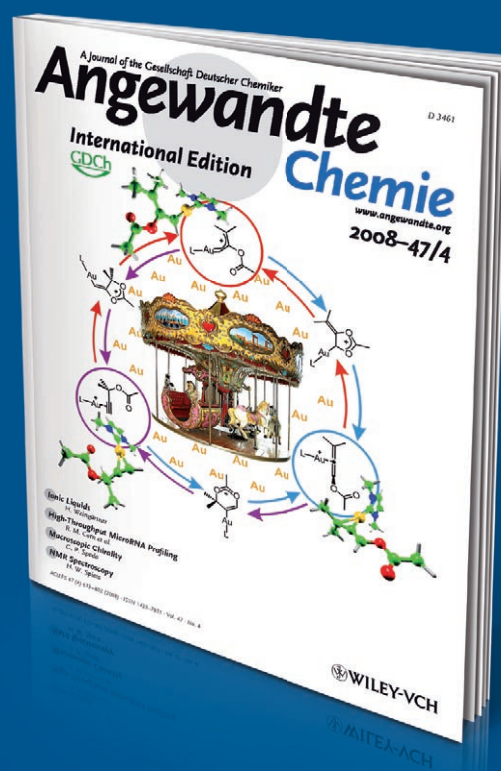
### Biomimetic Synthesis

S. Kang, J. Lucon, Z. B. Varpness, L. Liepold, M. Uchida, D. Willits, M. Young,\* T. Douglas\* 7845–7848

Monitoring Biomimetic Platinum Nanocluster Formation Using Mass Spectrometry and Cluster-Dependent H<sub>2</sub> Production



# Incredibly swift



Manuscripts submitted to *Angewandte Chemie* can be published in a matter of days, and that's including meticulous peer review, careful copy-editing, and author proofing. **The peer-review process requires an average of just 13 days, and 30% of all Communications are brought to readers within two months after submission of the original manuscript.** The articles are not only published rapidly, they are also swiftly assimilated within the scientific community, as reflected by the extremely high Immediacy Index of *Angewandte Chemie* (2007: 2.271).



GESELLSCHAFT DEUTSCHER CHEMIKER

[www.angewandte.org](http://www.angewandte.org)  
[service@wiley-vch.de](mailto:service@wiley-vch.de)

 **WILEY-VCH**



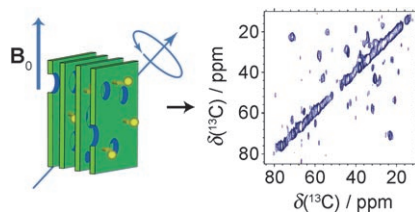


## Protein Structures

J. Xu, U. H. N. Dürr, S.-C. Im, Z. Gan,  
L. Waskell,  
A. Ramamoorthy\* — 7864–7867



Bicelle-Enabled Structural Studies on a  
Membrane-Associated Cytochrome  $b_5$  by  
Solid-State MAS NMR Spectroscopy



**Spinning bicelles:** Solving 3D structures of membrane proteins is a great challenge because of the difficulty in finding well-behaved model membranes. Bicelles are well suited to overcome these difficulties and enable the use of solid-state MAS NMR spectroscopy experiments for studies on a large soluble domain containing a low concentration of membrane protein cytochrome  $b_5$  at 37°C.

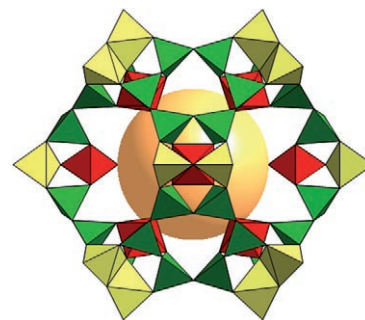
## Germanates

Q. Pan, J. Li, K. E. Christensen,  
C. Bonneau, X. Ren, L. Shi, J. Sun, X. Zou,\*  
G. Li, J. Yu,\* R. Xu — 7868–7871



A Germanate Built from a  $6^812^6$  Cavity  
Cotemplated by an  $(\text{H}_2\text{O})_{16}$  Cluster and  
2-Methylpiperazine

**Totally tubular:** A new tubular germanate is cotemplated by 2-methylpiperazine and an  $(\text{H}_2\text{O})_{16}$  cluster in a hydro(solvo)-thermal synthesis. The germanate features a large, highly symmetric  $6^812^6$  cavity (see picture; yellow sphere) built from 12  $\text{Ge}_7\text{X}_{19}$  ( $\text{X}=\text{O}, \text{OH}, \text{F}$ ) clusters ( $\text{GeX}_6$  red,  $\text{GeX}_5$  yellow,  $\text{GeX}_4$  green).

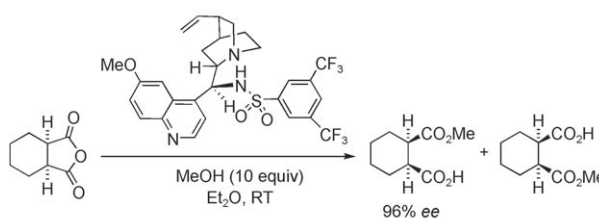


## Asymmetric Organocatalysis

S. H. Oh, H. S. Rho, J. W. Lee, J. E. Lee,  
S. H. Youk, J. Chin,\*  
C. E. Song\* — 7872–7875

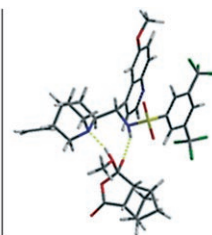


A Highly Reactive and Enantioselective  
Bifunctional Organocatalyst for the  
Methanolytic Desymmetrization of Cyclic  
Anhydrides: Prevention of Catalyst  
Aggregation



**Unprecedented reactivity** and high stereoselectivity were observed in the ring opening of *meso* anhydrides under mild conditions with a cinchona-alkaloid-based sulfonamide catalyst (see scheme). Com-

putation of the catalyst–transition-state analogue (right; gray C, white H, green F, blue N, red O, yellow S) provided insight into the origin of the stereoselectivity.

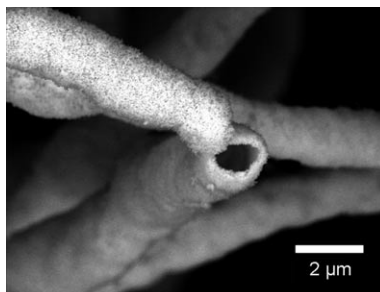


## Biotemplates for Nanotechnology

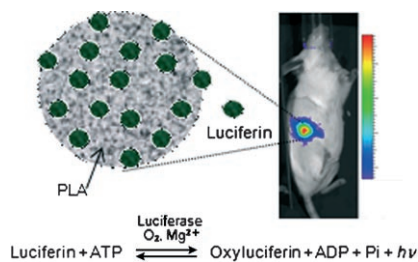
N. C. Bigall, M. Reitzig, W. Naumann,  
P. Simon, K.-H. van Pée,  
A. Eychmüller\* — 7876–7879



Fungal Templates for Noble-Metal  
Nanoparticles and Their Application in  
Catalysis



**Living templates:** Gold, silver, platinum, and palladium nanoparticles are synthesized. The as-obtained citrate-stabilized solutions are used as growth media for a variety of fungi. The nanoparticles partly assemble onto the mycelia, leading to a hybrid structure which consists of a biological template covered with nanoparticles. Supercritical drying of these structures conserves the three-dimensional tubular shape.

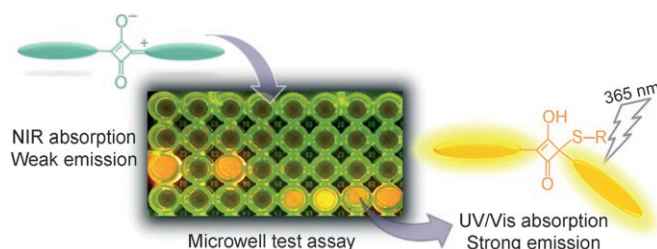


**Please release me:** Supercritical carbon dioxide was used as an antisolvent for the formation of nanoparticles that contain luciferin, a bioactive therapeutic, dispersed in poly(lactic acid) (PLA), a biodegradable polymer. These nanoparticles undergo slow and sustained drug release, which can be monitored by bioluminescence both in vitro and in vivo (see picture; ATP = adenosine triphosphate; ADP = adenosine diphosphate;  $\text{P}_i$  = inorganic phosphate).

### Drug Delivery

G. B. Jacobson, R. Shinde, C. H. Contag, R. N. Zare\* **7880–7882**

Sustained Release of Drugs Dispersed in Polymer Nanoparticles



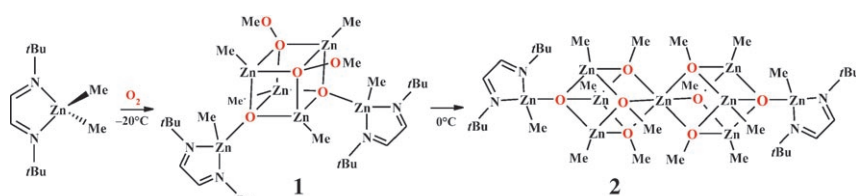
**Hunt for thiols:** A nucleophilic thiol attack on a weakly fluorescent near-infrared (NIR) squaraine dye results in a conjugation break to form an adduct that absorbs in the UV/Vis region and is highly fluorescent. This fluorophore allows the selec-

tive detection of thiols either by colorimetry or fluorescence (see picture). The probe is suitable for the detection and estimation of the total aminothiols content in human blood plasma.

### Molecular Probes

S. Sreejith, K. P. Divya, A. Ajayaghosh\* **7883–7887**

A Near-Infrared Squaraine Dye as a Latent Ratiometric Fluorophore for the Detection of Amino Thiol Content in Blood Plasma



**O what a reaction:** The oxygenation of  $\text{Me}_2\text{Zn} \cdot t\text{Bu-DAB}$  ( $t\text{Bu-DAB}$  = 1,4-di-*tert*-butyl-1,4-diazabutadiene) affords the unprecedented oxo(methylperoxide) cubane **1**, the corresponding double cubic

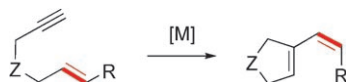
oxo(methoxide) **2**, and the C–C coupled dinuclear methoxide  $[(\text{MeZn})_2(t\text{Bu-DAB-DAB(H)}-t\text{Bu})(\mu\text{-OMe})]$ , the formation of which involves initial  $\text{ZnO-OMe}$  bond homolysis.

### Radical Reactions

J. Lewiński,\* K. Suwała, M. Kubisiak, Z. Ochal, I. Justyniak, J. Lipkowski **7888–7891**

Oxygenation of a  $\text{Me}_2\text{Zn}/\alpha$ -Diimine System: A Unique Zinc Methylperoxide Cluster and Evidence for Its Sequential Decomposition Pathways

**A skeleton in the closet:** The unprecedented title rearrangement of 1,6-enynes has been observed with gold and platinum catalysts (see scheme,  $[\text{M}]$  = metal catalyst,  $\text{Z} = \text{C}(\text{CO}_2\text{Me})_2$ ,  $\text{R}$  = electron-donating group). This reaction is proposed to proceed through an open carbocationic species.



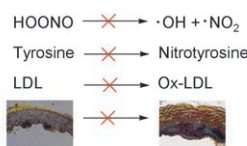
### Cycloisomerization Reactions

E. Jiménez-Núñez, C. K. Claverie, C. Bour, D. J. Cárdenas, A. M. Echavarren\* **7892–7895**

*cis*-Selective Single-Cleavage Skeletal Rearrangement of 1,6-Enynes Reveals the Multifaceted Character of the Intermediates in Metal-Catalyzed Cycloisomerizations

## Catalytic Antioxidants

A. Haber, A. Mohammed, B. Fuhrman,  
N. Volkova, R. Coleman, T. Hayek,  
M. Aviram,\* Z. Gross\* — 7896–7900



1-Fe > 1-Mn  
1-Mn, but not 1-Fe  
1-Fe, but not 1-Mn  
1-Fe > 1-Mn



Amphiphilic/Bipolar Metallocorroles That Catalyze the Decomposition of Reactive Oxygen and Nitrogen Species, Rescue Lipoproteins from Oxidative Damage, and Attenuate Atherosclerosis in Mice

**Antioxidants that work!** The iron corrole **1-Fe** (see picture) is a potent catalyst for decomposition of reactive oxygen and nitrogen species that binds selectively to lipoproteins. The complex also affects

cholesterol levels and its cellular efflux. **1-Fe** is more effective than natural antioxidants in reducing atherosclerosis development in mice. LDL = low-density lipoprotein.

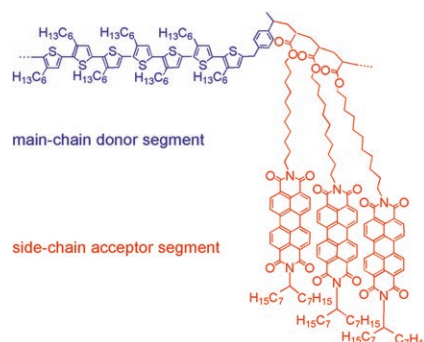
## Donor–Acceptor Block Copolymers

M. Sommer, A. S. Lang,  
M. Thelakkat\* — 7901–7904



Crystalline–Crystalline Donor–Acceptor Block Copolymers

**Efficient combination** of two polymerization reactions allowed various complex issues in photovoltaic devices, such as light absorption, the presence of a donor–acceptor heterojunction, photoluminescence quenching, crystallinity, and micro-phase separation, to all be addressed in a single block copolymer (see picture).

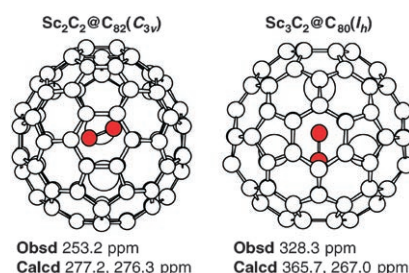


## Endohedral Fullerenes

Y. Yamazaki, K. Nakajima, T. Wakahara,  
T. Tsuchiya, M. O. Ishitsuka, Y. Maeda,  
T. Akasaka,\* M. Waelchli, N. Mizorogi,  
S. Nagase\* — 7905–7908



Observation of  $^{13}\text{C}$  NMR Chemical Shifts of Metal Carbides Encapsulated in Fullerenes:  $\text{Sc}_2\text{C}_2@C_{82}$ ,  $\text{Sc}_2\text{C}_2@C_{84}$ , and  $\text{Sc}_3\text{C}_2@C_{80}$



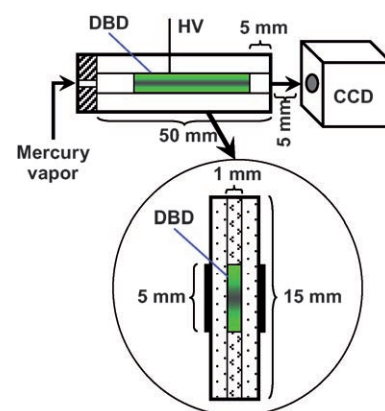
**Seeing the filling in fullerenes:** The  $^{13}\text{C}$  NMR chemical shifts of the  $\text{C}_2$  units in  $\text{Sc}_2\text{C}_2@C_{82}(\text{C}_{3v})$ ,  $\text{Sc}_2\text{C}_2@C_{84}(\text{D}_{2d})$ ,  $[\text{Sc}_3\text{C}_2@C_{80}(\text{I}_h)]^-$  (see picture), adamantylidene adduct of  $\text{Sc}_3\text{C}_2@C_{80}(\text{I}_h)$  were observed for the first time and agree well with the calculated values. The  $^{13}\text{C}$  NMR chemical shifts of all cage carbon atoms in these fullerenes were assigned by 2D INADEQUATE NMR measurements.

## Emission Spectrometry

Y.-L. Yu, Z. Du, M.-L. Chen,  
J.-H. Wang\* — 7909–7912

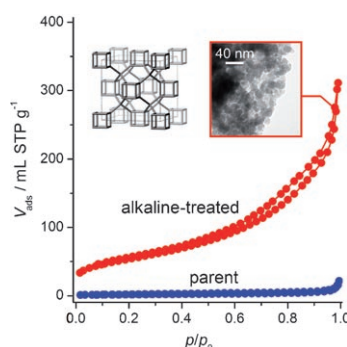
Atmospheric-Pressure Dielectric-Barrier Discharge as a Radiation Source for Optical Emission Spectrometry

**Honey, I shrunk the spectrometer:** The use of atmospheric-pressure dielectric-barrier discharge (DBD) as a radiation source for atomic optical emission spectrometry (OES) allowed the construction of a miniaturized DBD–OES system. A microsequential injection configuration (the picture shows the DBD unit and its cross-sectional configuration, HV = discharge power) provides favorable analytical performance for the system, as demonstrated for the determination of mercury.





**Clathrasils go functional:** Nanosized octadecasil crystals with tunable size and variable Si/Al ratio have been synthesized by controlled desilication of the parent clathrasil in alkaline medium. Extremely small (10–25 nm) nanocrystals with high external surface area ( $200 \text{ m}^2 \text{ g}^{-1}$ ) and preserved crystallinity were attained (see picture). This result widens the scope of this class of materials, opening room for catalytic applications.



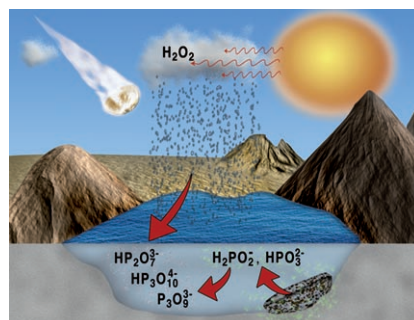
### Clathrates

J. Pérez-Ramírez,\* S. Abelló,  
L. A. Villaescusa, A. Bonilla **7913–7917**

Toward Functional Clathrasils: Size- and Composition-Controlled Octadecasil Nanocrystals by Desilication



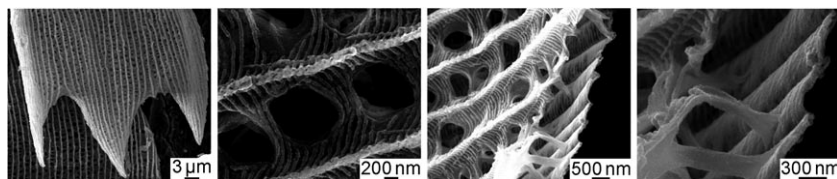
**Bringing phosphorus to life:** The prebiotic origin of key biomolecules such as RNA and ATP is contingent on a source of condensed phosphates, such as pyrophosphate and triphosphate. Condensed phosphates can be produced at high yields from the oxidation of H-phosphonate or H-phosphinate. Reactive phosphates were likely abundant on the early earth's surface, setting the stage for prebiotic chemistry that led to the evolution of life.



### Prebiotic Chemistry

M. A. Pasek,\* T. P. Kee, D. E. Bryant,  
A. A. Pavlov, J. I. Lunine **7918–7920**

Production of Potentially Prebiotic Condensed Phosphates by Phosphorus Redox Chemistry



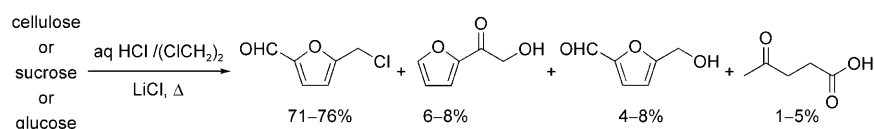
**Rutile replicas of butterfly scales:** Rutile titania-based structures, retaining the morphology of wing scales of a *Morpho* butterfly (see pictures), are synthesized using an automated, surface sol-gel process. By doping a titanium alkoxide pre-

cursor solution with a tin alkoxide, rutile structures were formed at 450 °C. This method may be used to apply rutile coatings on other organic templates for biomedical, filtration, or optical applications.

### 3D Nanostructures

M. R. Weatherspoon, Y. Cai, M. Crne,  
M. Srinivasarao,\*  
K. H. Sandhage\* **7921–7923**

3D Rutile Titania-Based Structures with *Morpho* Butterfly Wing Scale Morphologies



**Fueling up with furans:** Cellulose can be converted into furanic biofuels in unprecedented yields using an inexpensive, simple process involving concurrent hydrolysis, dehydration, and chlorine substitution reactions coupled with con-

tinuous extraction into an organic phase (see scheme). Furanic ethers, such as those that can be derived from the products above, are known diesel additives.

### Biofuels

M. Mascal,\* E. B. Nikitin **7924–7926**

Direct, High-Yield Conversion of Cellulose into Biofuel

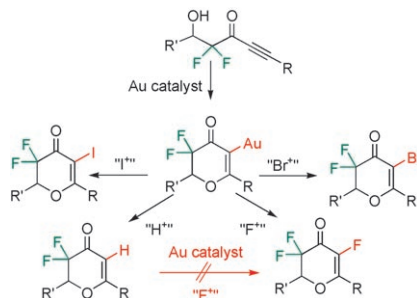


## Homogeneous Catalysis

M. Schuler, F. Silva, C. Bobbio, A. Tessier, V. Gouverneur\* — 7927 – 7930



Gold(I)-Catalyzed Alkoxyhalogenation of  $\beta$ -Hydroxy- $\alpha,\alpha$ -Difluoroyones



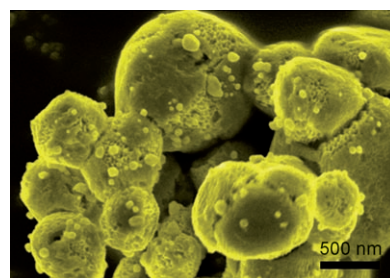
**Gold standard:** AuCl was found to be the only suitable catalyst for the 6-endo-dig ring closure of hydroxylated difluorinated ynone (see scheme), a class of substrates that displays low reactivity owing to the presence of the *gem*-difluoro group. For the first time, a gold catalyst is used in combination with an electrophilic fluorinating reagent.

## Photocatalysts

P. Wang, B. Huang,\* X. Qin, X. Zhang, Y. Dai, J. Wei, M.-H. Whangbo — 7931 – 7933

Ag@AgCl: A Highly Efficient and Stable Photocatalyst Active under Visible Light

**Plasmonic photocatalyst Ag@AgCl**, in which Ag nanoparticles are deposited on the surfaces of AgCl particles (SEM image depicted), was prepared by treating  $\text{Ag}_2\text{MoO}_4$  with HCl to form AgCl powder and then reducing some  $\text{Ag}^+$  ions in the surface region of the AgCl particles to  $\text{Ag}^0$ . This photocatalyst is highly efficient, for example in the degradation of organic dyes, and stable under visible light.

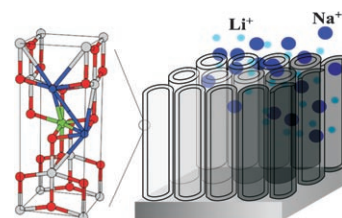


## Intercalation

A. Ghicov, M. Yamamoto, P. Schmuki\* — 7934 – 7937



Lattice Widening in Niobium-Doped  $\text{TiO}_2$  Nanotubes: Efficient Ion Intercalation and Swift Electrochromic Contrast



**Widely accommodating:** Novel  $\text{TiO}_2/\text{Nb}$  nanotube layers (see picture, right) are grown on a titanium–niobium alloy. Niobium doping of  $\text{TiO}_2$  enlarges the cell parameters of the anatase lattice (left; Nb green, Ti gray, O red), facilitating the intercalation of  $\text{H}^+$  and  $\text{Li}^+$  ions, and even larger  $\text{Na}^+$  ions (blue) into the lattice.

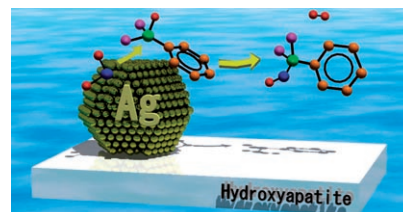
## Heterogeneous Catalysis

T. Mitsudome, S. Arita, H. Mori, T. Mizugaki, K. Jitsukawa, K. Kaneda\* — 7938 – 7940



Supported Silver-Nanoparticle-Catalyzed Highly Efficient Aqueous Oxidation of Phenylsilanes to Silanols

**Bon Apatite!** Hydroxyapatite-supported silver nanoparticles act as a highly efficient heterogeneous catalyst for the oxidation of diverse phenylsilanes into silanols in water (see picture; C orange, H red, O blue, R purple, Si green), while suppressing significant condensation to the disiloxanes. The solid silver catalyst is readily reusable without any loss of activity or selectivity.

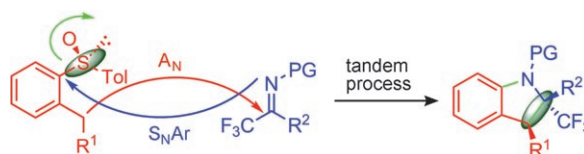


## Asymmetric Synthesis

J. L. García Ruano,\* J. Alemán, S. Catalán, V. Marcos, S. Monteagudo, A. Parra, C. del Pozo, S. Fustero\* — 7941 – 7944

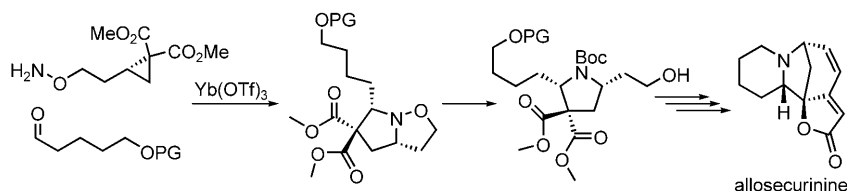


Anionic–Anionic Asymmetric Tandem Reactions: One-Pot Synthesis of Optically Pure Fluorinated Indolines from 2-*p*-Tolylsulfanyl Alkylbenzenes



**Chirality switch up:** A novel strategy has been developed to give optically pure fluorinated indolines with one or two stereogenic centers (see scheme;  $\text{A}_\text{N}$  = nucleophilic addition, PG = protect-

ing group,  $\text{S}_\text{N}\text{Ar}$  = intramolecular nucleophilic aromatic substitution, Tol = tolyl). Almost complete stereoselectivity and mild reaction conditions are the key features of the title reaction.



## Natural Products

A. B. Leduc, M. A. Kerr\* — 7945–7948

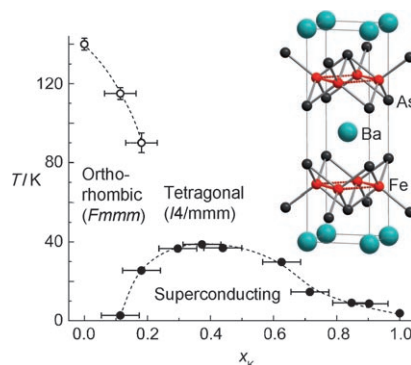
Total Synthesis of (–)-Allosecurinine



**Safe and secure:** An efficient methodology which provides access to homochiral 2,5-*cis* pyrrolidines in excellent yields starting from chiral alkoxyamine cyclopropanes was used in the total synthesis of (–)-

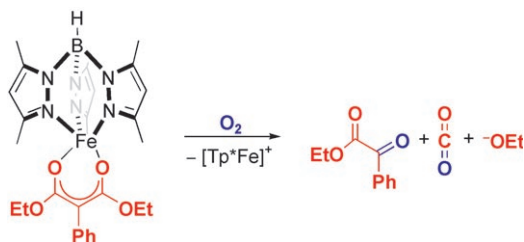
allosecurinine (see scheme). The synthesis proceeds with enantiomeric purity in 15 steps with an overall yield of 5%. OTf: trifluoromethanesulfonate, Boc: *tert*-butoxycarbonyl, PG: protecting group.

**Doping improves performance:** Iron arsenides ( $\text{Ba}_{1-x}\text{K}_x$ ) $\text{Fe}_2\text{As}_2$  with the  $\text{ThCr}_2\text{Si}_2$ -type structure exhibit superconductivity at 3–38 K depending on the potassium doping level. Superconductivity occurs before the structural distortion of the parent compound  $\text{BaFe}_2\text{As}_2$  ( $x=0$ ) is completely suppressed by doping (see phase diagram; ● critical temperature, ○ phase-transition temperature). Doping decreases the bond angles in the iron arsenide layers, suggesting a strong coupling of structural and electronic degrees of freedom.



## Superconductivity

M. Rotter, M. Pangerl, M. Tegel, D. Johrendt\* — 7949–7952

Superconductivity and Crystal Structures of ( $\text{Ba}_{1-x}\text{K}_x$ ) $\text{Fe}_2\text{As}_2$  ( $x=0-1$ )


**Position available:** A pentacoordinate iron(II) complex that binds and activates dioxygen shows dioxygenase activity and cleaves diethyl phenylmalonate, in ana-

logy to acetylacetone dioxygenase (see scheme). The mechanism for the model compound allows interesting hypotheses to be made about the enzyme function.

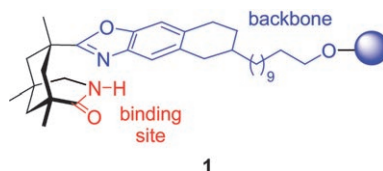
## Biomimetic O<sub>2</sub> Activation

I. Siewert, C. Limberg\* — 7953–7956

A Trispyrazolylborato Iron Malonate Complex as a Functional Model for the Acetylacetone Dioxygenase



**A happy couple:** A chiral complexing agent was modified with an  $\omega$ -hydroxyalkyl linker and immobilized on a Wang resin and on a methoxypolyethylene glycol (MPEG 2000). The immobilized templates **1** served in an enantioselective photochemical reaction with impressive selectivity (e.r. 92:8 to 96:4) and stability over several cycles.



## Photochemical Synthesis

S. Breitenlechner, T. Bach\* — 7957–7959

A Polymer-Bound Chiral Template for Enantioselective Photochemical Reactions


Supporting information is available on [www.angewandte.org](http://www.angewandte.org) (see article for access details).

A video clip is available as Supporting Information on [www.angewandte.org](http://www.angewandte.org) (see article for access details).

# Sources

## Product and Company Directory

You can start the entry for your company in "Sources" in any issue of *Angewandte Chemie*.

If you would like more information, please do not hesitate to contact us.

Wiley-VCH Verlag – Advertising Department

Tel.: ☎ 62 01 - 60 65 65

Fax: ☎ 62 01 - 60 65 50

E-Mail: MSchulz@wiley-vch.de

## Service

Spotlights Angewandte's

Sister Journals \_\_\_\_\_ 7792 – 7793

Keywords \_\_\_\_\_ 7962

Authors \_\_\_\_\_ 7963

Sources \_\_\_\_\_ A65

Preview \_\_\_\_\_ 7965

## Corrigendum

N-Terminal Protein Modification through a Biomimetic Transamination Reaction

J. M. Gilmore, R. A. Scheck,  
A. P. Esser-Kahn, N. S. Joshi,  
M. B. Francis\* \_\_\_\_\_ 5307–5311

*Angew. Chem. Int. Ed.* **2006**, 45

DOI 10.1002/anie.200600368

In Figure 1 b of this Communication, the signal corresponding to unmodified myoglobin is incorrectly labeled with  $m/z$  16992. The Figure with the correct value of  $m/z$  16962 is given here.

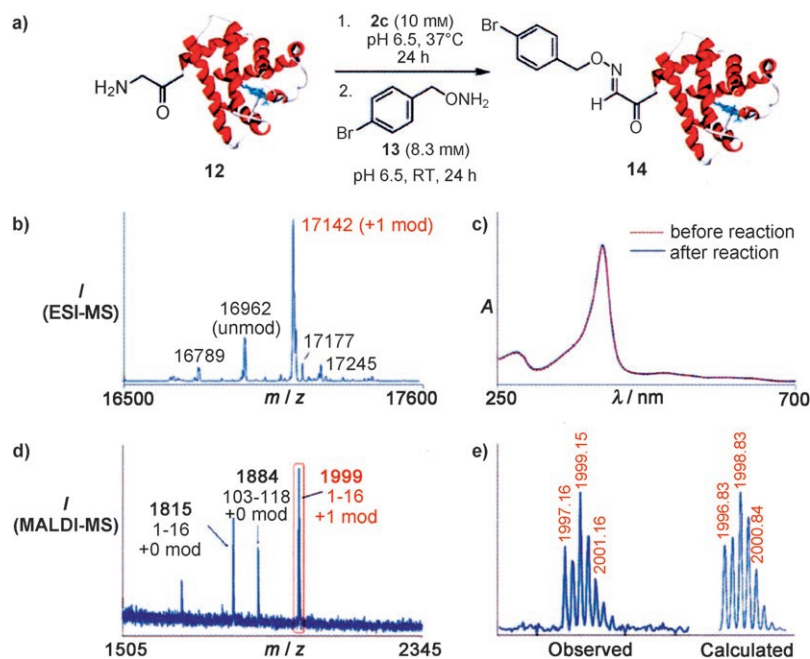


**Figure 1.** Site-selective protein modification with PLP. a) Myoglobin was treated with **2c** at 37°C for 24 h. After removal of small molecules by gel filtration, oxime **14** was formed after reaction with **13**. b) ESI-LCMS studies indicated that only one modification had occurred. c) UV/Vis spectra of **12** subjected to the reaction conditions in the absence (dotted red) and presence (dashed blue) of **2c**. d) Product **14** was digested with trypsin, and the resulting fragments were analyzed by MALDI-TOF MS. The only modified fragment observed contained the N-terminal residue. e) Predicted (left) and observed (right) isotope patterns for the modified myoglobin peptide fragment shown in (d). All MS values agree with those predicted within 0.01%.